Macromolecular Research, Vol. 16, No. 6, pp 555-560 (2008)

Gas Permeation Properties of Hydroxyl-Group Containing Polyimide Membranes

Chul Ho Jung and Young Moo Lee*

School of Chemical Engineering, College of Engineering, Hanyang University, Seoul 133-791, Korea

Received February 9, 2008; Revised March 26, 2008; Accepted March 26, 2008

Abstract: A series of hydroxyl-group containing polyimides (HPIs) were prepared in order to investigate the structure-gas permeation property relationship. Each polymer membrane had structural characteristics that varied according to the dianhydride monomers. The imidization processes were monitored using spectroscopic and thermog-ravimetric analyses. The single gas permeability of He, H_2, CO_2, O_2, N_2 and CH_4 were measured and compared in order to determine the effect of the polymer structure and functional -OH groups on the gas transport properties. Surprisingly, the ideal selectivity of CO_2/CH_4 and H_2/CH_4 increased with increasing level of -OH incorporation, which affected the diffusion of H_2 or the solubility of CO_2 in HPIs. For H_2/CH_4 separation, the difference in the diffusion coefficients of H_2 and CH_4 was the main factor for improving the performance without showing any changes in the solubility coefficients. However, the solubility coefficient of CO_2 in the HPIs increased at least four fold compared with the conventional polyimide membranes depending on the polymer structures. Based on these results, the polymer membranes modified with -OH groups in the polymer backbone showed favorable gas permeation and separation performance.

Keywords: gas separation, polyimide, hydroxyl group, diffusion coefficient, solubility coefficient.

Introduction

Over the past several decades, membrane processes have focused on gas separation applications resulting in advantages in various areas such as energy and cost effectiveness.[1,2] Nonetheless, superior membrane materials exhibiting high gas selectivity and permeability are required for successful application to typical separation processes.[3] Criteria for selecting membranes for a given application are complex; durability, mechanical integrity at operating conditions, productivity and separation efficiency are important factors that must be balanced against cost.[4-6] Selectivity and permeation rate are important requirements for membrane selection.

Among the various membrane materials used for gas separation, aromatic polyimides are a class of high-performance polymers that have a high thermal stability, high glass-transition temperatures, and relatively low dielectric constants. In addition, membranes rendered from polyimides have shown impressive performance for separating gas mixtures such as O_2/N_2 and CO_2/CH_4. Various research has investigated the preparation of functionalized polyimides for manifold applications such as carbon membrane precursors,[7,8] fuel cell membranes,[9] nonlinear optical (NLO) applications,[10-12] and gas separation membranes.[13-15]

Hydroxyl-group containing polyimides (HPIs) have been primarily used for NLO chromophores due to their large electro-optic coefficients, low dielectric constants, and flexibility in fabrication.[16,17] HPIs as membrane materials have many advantages resulting from their polar structures. 6F-based polyimides containing polar hydroxyl groups were studied to render thin skin layers for asymmetric hollow fiber composite membranes.[18] The hexafluroisopropylidene ($-C(CF_3)_2-$) group provides high solubility of the resulting polymers in common organic solvents.[18,19] HPIs can be dissolved in general coating solvents such as alcohol. As reported recently by our group, HPIs can be thermally converted to a polybenzoxazole group which showed excellent CO_2 separation performance over conventional polymer membranes.[18-20] However, there have been no studies on the effect of functional hydroxyl and bridging groups in HPI on gas permeation properties.

The objective of this study was to investigate the gas permeation and diffusion properties of HPIs with various structures and to compare them with common PI membranes. 2,2-bis(3-amino-4-hydroxy-phenyl) hexafluoropropane (APAF) with a pair of hydroxyl groups at the ortho position of amine group was selected as the diamine monomer.

Experimental

Polymer Synthesis and Membrane Formation. As shown in Figure 1, five hydroxyl polyimides were synthesized

*Corresponding Author. E-mail: ymlee@hanyang.ac.kr

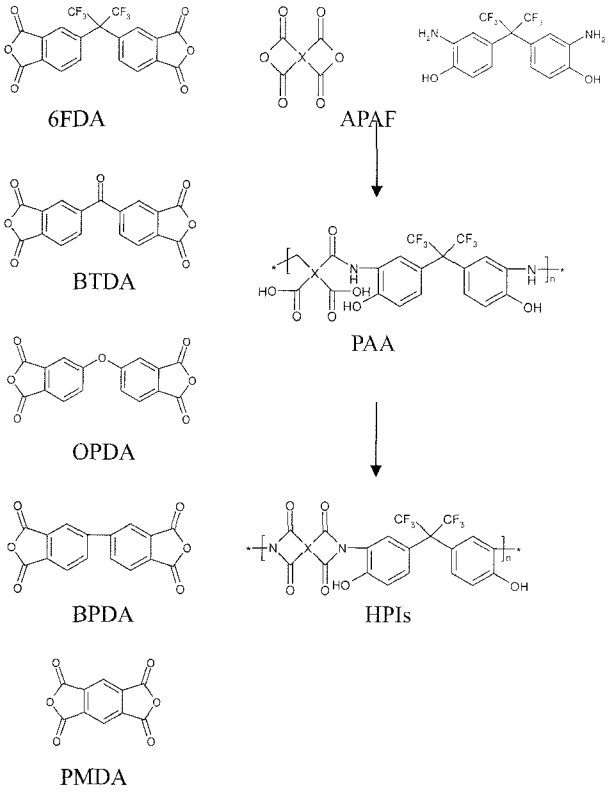

Figure 1. Chemical structures of used monomers and thermal imidization scheme.

using 4,4'-(hexafluroisopropylidene)-diphthalic anhydride (6FDA), 4,4'-oxydiphthalic anhydride (OPDA), 3,3',4,4'-biphenyltetracarboxylic dianhydride (BPDA), pyromellitic anhydride (PMDA) and benzophenone-3,3,4,4,-tetracarboxylic anhydride (BTDA). 6FDA, OPDA, BPDA, PMDA and BTDA were obtained from Aldrich (Milwaukee, WI, USA) and APAF was purchased from Tokyo Kasei Co., Inc. (Tokyo, Japan). The dianhydride and diamine monomers were purified by vacuum sublimation or repeat crystallization immediately prior to polymerization. N-methyl-2-pyrrolidinone (NMP) purchased from Aldrich was used as a solvent and was stirred over CaH_2 overnight and distilled under reduced pressure. NMP was stored over 4 Å molecular sieves in nitrogen. Five poly(amic acids) were synthesized to prepare HPIs membranes. For example, 50 mL of NMP was introduced into a 250-mL three-neck flask under N_2 flow. Next, 10 mmols of APAF was dissolved, and equimolar 6FDA was added drop-wise, resulting in a clear yellowish PAA solution after six hours of stirring. All other HPIs were prepared using the same procedure. In addition, a polyimide membrane was prepared via the same procedure from 2,2-bis(3-aminophenyl)-hexafluoropropane and 6FDA to compare the effect of -OH functional groups.

All polyimides were prepared via a conventional two-step polycondensation technique with thermal imidization of the PAAs. PAA solutions were cast onto a glass plate and thermally imidized in a vacuum oven with precise temperature control up to 250 °C as previously reported. Casted membranes showed a high affinity to a glass plate due to strong interaction (e.g., hydrogen bonding) between hydroxyl groups on the glass plate and -OH functional groups in the polymer matrix. As a result, the virgin membranes were carefully peeled off in a hot distilled water bath. Prepared membranes were stored in a desiccator containing dry silica gel to avoid the influence of humidity.

Characterization of Membrane Samples. Attenuated total reflection Fourier transform infrared (ATR-FTIR) spectra of samples were acquired using an infrared microspectrometer (IlluminatIR, SensIR Technologies, Danbury, CT, USA). Thermogravimetric analysis was performed using TG209F1 (NETZSCH, Germany) to monitor the stability of HPI samples. X-ray diffraction patterns were measured using a wide-angle X-ray diffractometer (D/MAX-2500, Rigaku, Japan) operating in a 2-theta range of 5-60° with a scan rate of 5°/min. The density of HPI membranes was measured by a top-loading electronic Mettler Toledo balance coupled with a density kit based on Archimedes' principle. The samples were weighed in air and a known-density liquid, a high purity water. The measurement was performed at room temperature by the buoyancy method and the density was calculated as follows:

$$\rho_{membrane} = \frac{w_0}{w_0 - w_1}\rho_{liquid} \quad (1)$$

where w_0 and w_1 are the membrane weights in air and water, respectively.

Measurement of Gas Separation Performance. The permeation properties of HPI membranes were analyzed with different kinetic diameters of gas molecules: He (2.6 Å), H_2 (2.89 Å), CO_2 (3.3 Å), O_2 (3.46 Å), N_2 (3.64 Å), and CH_4 (3.80 Å). Gas permeability was determined by the time-lag method at a feed pressure of 760 Torr and temperature of 25 °C. Before the gas permeation test, permeation sides were thoroughly evacuated to below 10^{-5} Torr. The pressure rise versus the time transient of the permeate side equipped with a pressure transducer (MKS Baratron type 146, MA, USA) was recorded and sent to a desktop computer through a RS-232 cable. The permeability, P, was obtained from the steady-state permeation rate, R, as

$$P = \frac{R/A}{\Delta p/l} \quad (2)$$

where A and l are the effective membrane area (cm^2) and membrane thickness (cm), respectively. Δp (cmHg) is the pressure difference between the feed (760 Torr) and permeate side ($< 1\times10^{-5}$ Torr). The ideal separation factor (gas selectivity) for components 1 and 2 is defined as the ratio of the pure gas permeabilities of each component:

$$\alpha_{1/2} = \frac{P_1}{P_2} \quad (3)$$

Results and Discussion

Characterization of HPI Membranes. ATR-FTIR was used to confirm the imidization of HPI membranes and the chemical structure of five HPI series. As shown in Figure 2, the absorption band at 1680 cm^{-1} of C=O stretching in the COOH of PAA became two characteristic bands at 1778 and 1730 cm^{-1} of the imide C=O stretching linkage. In addition, an absorption band at 1370 cm^{-1} (CNC stretching) was observed, while a band at 1569 cm^{-1} (NH stretching) disappeared after thermal imidization. The characteristic peaks of the C-F bonds stretched at 1246, 1196, and 1151 cm^{-1} because the hexafluoroisopropylidene group of the APAF moiety and -OH group peaks appeared at 3500 cm^{-1}. These peaks clearly indicated the existence of imide groups and confirmed the successful preparation of HPI membranes.

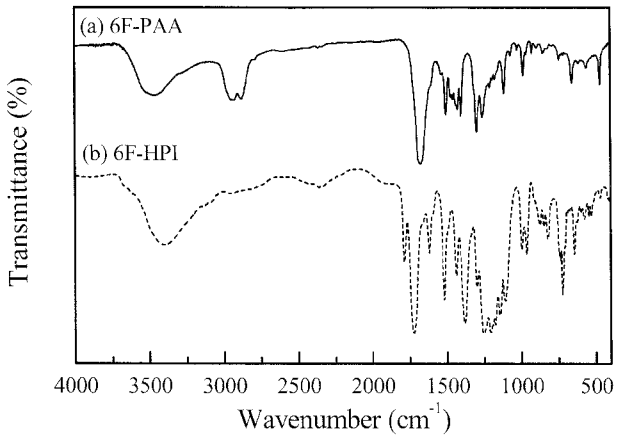

Figure 2. FT IR spectroscopy of (a) 6F-PAA and (b) 6F-HPI.

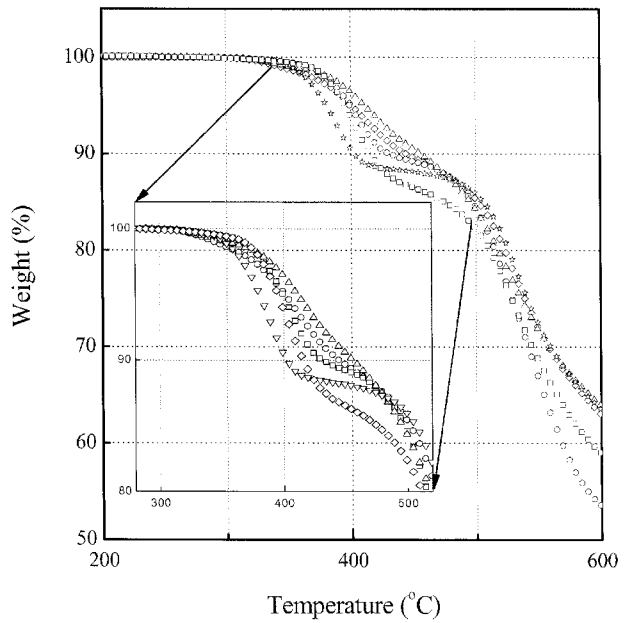

Figure 3. TGA thermogram of HPI membranes: (○) 6F-HPI, (□) P-HPI, (△) B-HPI, (◇) Bt-HPI and (☆) O-HPI.

Table I. Weight Loss of HPI Membranes at 400-500 °C

	Theoretical	Experimental
P-HPI	15.8	13.7
6F-HPI	11.0	10.7
B-HPI	13.9	9.5
Bt-HPI	13.3	10.9
O-HPI	13.6	11.6

The TGA thermogram of the HPI membranes was measured under nitrogen and is shown in Figure 3. All of the HPI series were stable up to 400 °C, and the first weight loss was observed at 450 °C. At these temperatures, a polybenzoxazole structure formed due to a thermal rearrangement reaction.[21] The weight loss was summarized in Table I. Theoretically, P-HPI showed the highest weight loss, corroborating experimental results. However, the trends and shapes of the weight loss at 450 °C were similar for all HPI series, and the polymer backbone decomposed at temperatures greater than 500 °C.

Wide Angle X-ray Diffractions and Physical Properties. Wide angle X-ray diffraction (WAXD) can be used as a qualitative measurement of the differences in interlayer spacing. Regular ordered dimensions can be calculated from the Bragg equation,

$$n\lambda = 2d\sin\theta \tag{4}$$

where d is the d-spacing, ϕ is the diffraction angle, λ is the X-ray wavelength (1.54 Å), and n is an integral number (1,

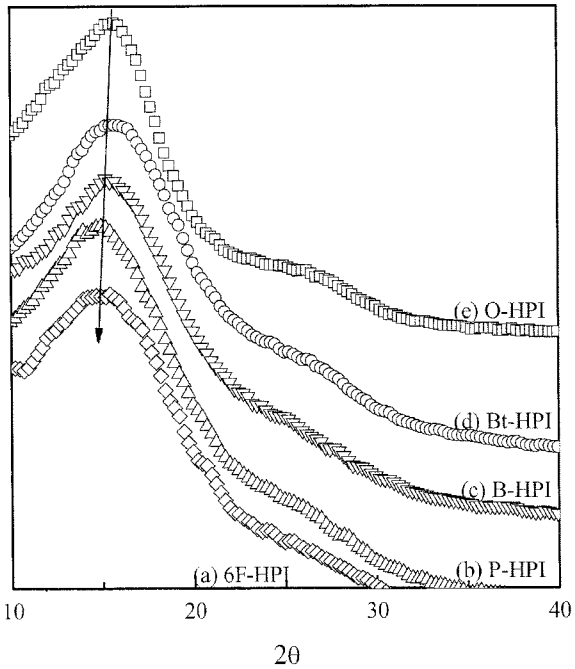

Figure 4. X-ray diffraction patterns of HPI membranes.

Table II. *d*-Spacing Values of HPI Membranes

Sample	*d*-Spacing (Å)
6F-HPI	6.06
P-HPI	5.66
B-HPI	5.98
Bt-HPI	5.79
O-HPI	5.71

2, 3, ···). Generally, X-ray diffraction is a useful tool for studying the inter-planar distances for amorphous glassy structures. The changes of *d*-spacing depend on the extent of heat treatment and can provide an indicator of the amount of available space to penetrate small molecules. Figure 4 and Table II show the X-ray diffraction patterns of HPI membranes. *d*-Spacings gradually decreased in the following order: 6F-HPI > P-HPI > B-HPI > Bt-HPI > O-HPI. Bulky hexafluoroisopropylidene moieties in 6F-HPI interrupt inter-chain packing, which can correlate with the high fractional free volume of 6F-HPI. *d*-Spacings of Bt- and O-HPI with carbonyl and ether bridging moieties showed lower values than without them. Secondary forces (e.g., hydrogen bonding) between the -OH group and bridging unit (e.g., carbonyl or ether linkage) may be a reason for decreasing *d*-spacing values in the HPIs.

Gas Separation Performance of HPI Membranes. The gas separation performance through HPI membranes was investigated at 25 °C for six single gas permeants with different kinetic diameters (He: 2.6 Å, H_2: 2.89 Å, CO_2: 3.3 Å, O_2: 3.46 Å, N_2: 3.64 Å and CH_4: 3.8 Å). The permeation properties of HPI membranes were investigated by varying the structures of the repeating units. The gas permeability and selectivity of HPI membranes are shown in Table VI. The permeability coefficients decreased in the following order:

$$He > H_2 > CO_2 > O_2 > N_2 > CH_4$$

which was also the order of increasing kinetic diameters of the gases.

Among the HPI membranes, the highest permeability was obtained from 6F-HPI due to the largest *d*-spacings, and the highest FFV was obtained from 6FDA and APAF(Table III). The $-C(CF_3)_2-$ of 6F-HPIs produced diffusive channels for the tested gases, suggesting that the introduction of $-C(CF_3)_2-$ linkages was very effective for improving permeability and permselectivity for tested gases. The permeability coefficients of HPI membranes decreased as follows: 6F-HPI > P-HPI > B-HPI > Bt-HPI > O-HPI.

These results coincided well with FFV and XRD pattern results. In particular, O-HPI showed the highest O_2/N_2, H_2/N_2, and H_2/CH_4 selectivities with the lowest gas permeability. The order of permeabilities of HPI membranes matched well with the data obtained from PI using the same anhydrides with 2,2-bis-(4-aminophenyl)hexafluoropropane (BAHF), which has the same structure of APAF, although hydroxyl groups are not attached to the amine group at the ortho position in the monomer.[22]

A comparison of the two types of polymer membranes

Table III. Physical Characteristics of HPI Membranes

	Density[a] (g/cm^3) Experimental	Density[b] (g/cm^3) Calculated	V (cm^3/g)	V_o (cm^3/g)	FFV
6F-HPI	1.55	1.587	0.630	0.432	0.109
P-HPI	1.54	1.544	0.629	0.444	0.082
B-HPI	1.47	1.505	0.664	0.456	0.107
Bt-HPI	1.49	1.512	0.661	0.454	0.107
O-HPI	1.50	1.512	0.661	0.452	0.112

[a]Density obtained from the buoyancy method. [b]Density calculated using the synthia module of the Accelrys MS modeling 4.0 program.

Table VI. Single Gas Permeability and Permselectivity of HPI Membranes

	He	H_2	CO_2	O_2	N_2	CH_4	O_2/N_2	CO_2/N_2	CO_2/CH_4	H_2/N_2	H_2/CH_4
	P (Barrer)[a]										
6F-HPI	67.85	42.75	16.95	3.73	0.55	0.21	6.8	31.0	79.5	78.0	200.1
P-HPI	62.21	35.21	9.87	2.58	0.36	0.08	7.1	27.3	121.4	97.4	433.0
B-HPI	23.57	14.26	2.74	0.72	0.09	0.03	7.7	29.5	90.6	153.5	470.9
Bt-HPI	19.75	11.13	1.43	0.60	0.08	0.02	6.6	17.9	71.5	139.1	556.5
O-HPI	23.45	13.36	1.81	0.54	0.06	0.02	9.3	31.5	107.6	231.8	792.3

[a]1 Barrer = 1×10^{-10} cm^3(STP)·cm/cm^2·s·cmHg.

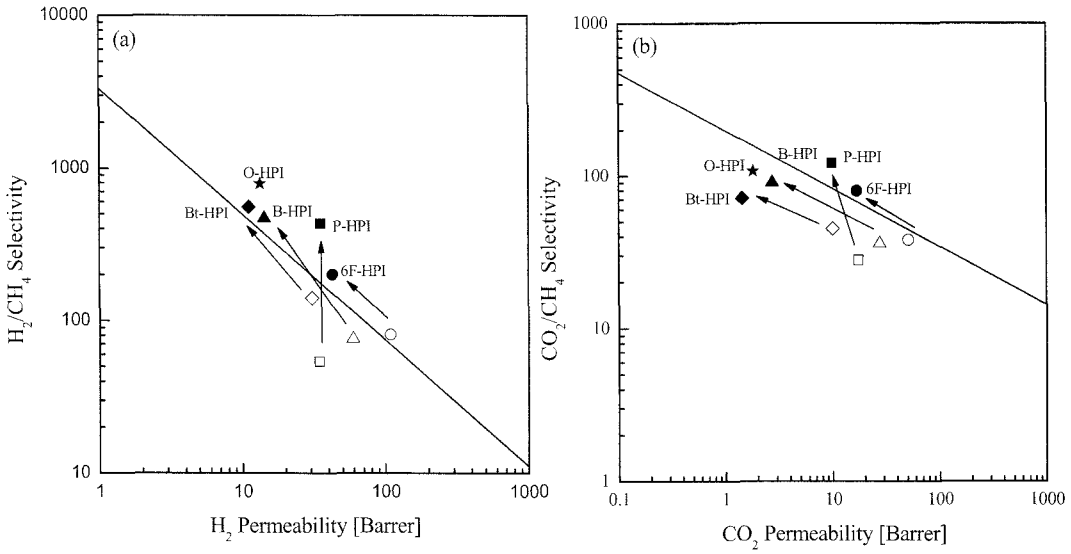

Figure 5. (a) H_2 permeability vs H_2/CH_4 selectivity and (b) CO_2 permeability vs CO_2/CH_4 selectivity (closed symbols: HPI membranes; open symbols: non-HPI membranes).

with and without -OH groups was used to understand the role of -OH groups in polymers for gas permeation. As shown in Figure 5, the gas selectivity of HPIs showed much higher values, particularly for the H_2/CH_4 and CO_2/CH_4 gas pairs. This result proves that the introduction of hydroxyl groups effectively increased the gas selectivity for H_2 and CO_2 separation from large gas molecules.

To investigate the gas transport mechanism of HPI membranes, diffusion and solubility coefficients were calculated and are listed in Table V. The -OH groups may contribute differently to improving H_2 and CO_2 separations. For H_2/CH_4 separation, an increase of diffusion selectivities was the contributing factor for higher H_2/CH_4 separation performance, suggesting that the H_2 diffusivity (D_{H2}) increased and CH_4 diffusivity (D_{CH4}) decreased with the incorporation of -OH groups in the polyimide backbone. For example, the D_{H2} of 6F-PI increased from 290 to 331×10^{-8} cm^2/s by incorporating -OH groups, and the D_{CH4} decreased from 0.660 to 0.091×10^{-8} cm^2/s. Therefore, D_{H2}/D_{CH4} of 6F-HPI was nine times higher than conventional 6F-PI. In contrast, the solubility coefficient of CO_2 was 4-6 times higher than that of the PI series due to the incorporation of -OH groups in the polyimide backbone. In general, polymers with the highest CO_2 solubility contain polar groups such as ether oxygens, nitriles, and acetates.[23] These groups are typically used to improve barrier properties by increasing chain rigidity and lowering diffusion coefficients. There was no distinct increase in the separation performance of polymers having polar

Table V. Diffusion Coefficients, Solubility Coefficients and Ratios of Each Coefficient for the H_2/CH_4 and CO_2/CH_4 Systems in HPI Membranes at 30 °C and 760 Torr

	Diffusion Coefficient (10^{-8} cm^2/s)			Solubility Coefficient (10^{-3} cm^3(STP)·cm/cmHg)			Diffusion Selectivity		Solubility Selectivity	
	D_{H2}	D_{CO2}	D_{CH4}	S_{H2}	S_{CO2}	S_{CH4}	D_{H2}/D_{CH4}	D_{CO2}/D_{CH4}	S_{H2}/S_{CH4}	S_{CO2}/S_{CH4}
6F-HPI	331	0.429	0.091	1.29	396	23	3637	4.7	0.30	17
P-HPI	257	0.387	0.041	1.40	255	20	6268	9.44	0.07	13
B-HPI	236	0.126	0.023	0.60	218	13	10261	5.48	0.05	17
Bt-HPI	144	0.080	0.021	0.77	180	14	6857	3.81	0.06	13
O-HPI	814	0.132	0.016	0.16	137	10	49634	8.05	0.02	14
6F-PI[a]	290	8.1	0.660	3.7	63	20	440	12	0.20	3.2
P-PI[a]	220	5.3	0.937	2.3	47	14	235	8	0.16	3.4
B-PI[a]	400	4.6	0.780	1.5	60	18	513	11	0.08	3.3
Bt-PI[a]	67	1.7	0.226	4.6	59	19	296	14	0.24	3.1

[a]Data were collected from the reference[18] for comparison.

groups due to the trade-off relationship between solubility and diffusion coefficients. However, for HPI membranes, an increase in CO_2/CH_4 solubility selectivity overwhelmed the decrease of diffusion selectivity due to the strong polar character of HPI. From these results, it may be concluded that the -OH groups were superior to the other polar groups in increasing CO_2 solubility selectivity. For these reasons, higher gas selectivities were obtained for H_2 and CO_2 gases than for nonpolar gases because of two different factors, namely diffusivity and solubility coefficients, respectively.

Conclusions

Five hydroxyl group containing polyimide membranes were prepared and characterized to investigate the structure-gas permeation property relationship and the effect of hydroxyl groups on gas separation properties. The molecular structure of the HPI membranes had a strong influence on the permeability coefficients of various tested gases. For He, H_2, CO_2, O_2, N_2 and CH_4, the HPI-series membranes showed higher gas selectivity than conventional PI membranes. The solubility of CO_2 in the HPI series significantly increased compared to that in the general PI series membranes since the hydroxyl groups aided in increasing the solubility coefficient of condensable gases, although a small decrease in gas diffusivity was also noticed. Modification of the polymer structure by incorporating hydroxyl groups in PI maximized the difference of the diffusivity coefficient between H_2 and CH_4 gas pairs and increased the H_2/CH_4 selectivity. For the H_2 and CO_2 separation process, the introduction of -OH groups was an effective method for improving gas separation performance.

Acknowledgements. This research was supported by a grant (DB2-101) from Carbon Dioxide Reduction & Sequestration Research Center, one of the 21st Century Frontier programs funded by the Ministry of Science and Technology of the Korean Government.

References

(1) S. A. Stern, *J. Membr. Sci.*, **94**, 1 (1994).
(2) W. J. Koros and G. K. Fleming, *J. Membr. Sci.*, **83**, 1 (1993).
(3) H. Kawakami, M. Mikawa, and S. Nagaoka, *J. Membr. Sci.*, **137**, 241 (1997).
(4) W. J. Koros and R. Mahajan, *J. Membr. Sci.*, **175**, 181 (2000).
(5) J. W. Rhim, S. H. Hwang, D. S. Kim, H. B. Park, C. H. Lee, Y. M. Lee, G. Y. Moon, and S. Y. Nam, *Macromol. Res.*, **13**, 135 (2005).
(6) S. W. Kang, J. H. Kim, and K. Char, Y. S. Kang, *Macromol. Res.*, **13**, 162 (2005).
(7) H. B. Park, I. Y. Suh, and Y. M. Lee, *Chem. Mater.*, **14**, 3034 (2002).
(8) H. B. Park and Y. M. Lee, *Adv. Mater.*, **17**, 477 (2005).
(9) C. H. Lee, H. B. Park, Y. S. Chung, Y. M. Lee, and B. D. Freeman, *Macromolecules*, **39**, 755 (2006).
(10) N. Song, L. Men, P. Gao, Y. Bai, A. M. R. Beaudin, G. Yu, and Z. Y. Wang, *Chem. Mater.*, **16**, 3708 (2004).
(11) A. Qin, Z. Yang, F. Bai, and C. Ye, *J. Polym. Sci. Polym. Chem.*, **41**, 2846 (2003).
(12) J. Y. Lee, J. H. Kim, and B. K. Rhee, *Macromol. Res.*, **15**, 234 (2007).
(13) S. H. Park, K. J. Kim, W. W. So, S. J. Moon, and S. B. Lee, *Macromol. Res.*, **11**, 157 (2003).
(14) M. D. Guiver, G. P. Robertson, Y. Dai, F. Bilodeau, Y. S. Kang, K. J. Lee, J. Y. Jho, and J. O. Won, *J. Polym. Sci. Polym. Chem.*, **40**, 4193 (2002).
(15) G. C. Eastmond, M. Gibas, W. F. Pacynko, and J. Paprotny, *J. Membr. Sci.*, **207**, 29 (2002).
(16) S. B. Mhaske, R. V. Bhingarkar, M. B. Sabne, R. Mercier, and S. P. Vernekar, *J. Appl. Polym. Sci.*, **77**, 627 (2000).
(17) W. N. Leng, Y. M. Zhou, Q. H. Xu, and J. Z. Liu, *Polymer*, **42**, 7749 (2001).
(18) K. J. Kim, S. H, Park, W. W. So, D. J. Ahn, and S. J. Moon, *J. Membr. Sci.*, **211**, 41 (2003).
(19) D. Likhatchev, C. Gutierrez-Wing, I. Kardash, and R. Vera-Graziano, *J. Appl. Polym. Sci.*, **59**, 725 (1996).
(20) H. B. Park, C. H. Jung, Y. M. Lee, A. J. Hill, S. J. Pas, S. T. Mudie, E. V. Wagner, B. D. Freeman, and D. J. Cookson, *Science*, **318**, 254 (2007).
(21) G. L. Tullos, J. M. Powers, S. J. Jeskey, and L. J. Mathias, *Macromolecules*, **32**, 3598 (1999).
(22) K. Tanaka, H. Kita, M. Okano, and K. Okamoto, *Polymer*, **33**, 585 (1992).
(23) L. H. Sperling, *Introduction to Physical Polymer Science*, Second Ed., Wiley, New York, 1992.